Staurosporine Inhibits Voltage-Dependent K^+ Current Through a PKC-Independent Mechanism in Isolated Coronary Arterial Smooth Muscle Cells

Won Sun Park, Youn Kyoung Son,* Jin Han,† Nari Kim,† Jae-Hong Ko,* Young Min Bae,‡ and Yung E. Earm**

Abstract: We examined the effects of the protein kinase C (PKC) inhibitor staurosporine (ST) on voltage-dependent K^+ (K_V) channels in rabbit coronary arterial smooth muscle cells. ST inhibited the K_V current in a dose-dependent manner with a K_d value of 1.3 μM. The inhibition of the K_V current by ST was voltage-dependent between −30 and +10 mV. The additive inhibition of the K_V current by ST was voltage-dependent throughout the activation voltage range. The rate constants of association and dissociation of ST were 0.63 μM^{-1} s^{-1} and 0.92 s^{-1}, respectively. ST produced use-dependent inhibition of the K_V current. ST shifted the activation curve to more positive potentials but did not have any significant effect on the voltage dependence of the inactivation curve. ST did not have any significant effects on other types of K^+ channel. Another PKC inhibitor, chelerythrine, and PKA inhibitor peptide (PKA-IP) had little effect on the K_V current. These results suggest that ST interacts with K_V channels that are in the closed state and that ST inhibits K_V channels in the open state in a manner that is phosphorylation-independent and voltage-, time-, and use-dependent.

Key Words: coronary arterial smooth muscle, voltage-dependent K^+ channel, protein kinase C, staurosporine, electrophysiology, open block

(*J Cardiovasc Pharmacol*™ 2005;45:260–269)

Protein kinase C (PKC) phosphorylates the hydroxyl groups of serine (Ser) and/or threonine (Thr) residues in numerous proteins. Activation of PKC is one of the earliest events in the cascade of signal transduction pathways that leads to a variety of cellular responses, including cellular growth, differentiation, secretion, gene expression, and proliferation.[1–5] In vascular tissues, PKC can induce several important effects, such as smooth muscle cell proliferation, reactive oxygen species–induced cell apoptosis, contraction, and modulation of ion channels.[6–8] Ion channels are important targets for PKC-mediated signaling pathways. For example, the activity of L-type Ca^{2+} channels and store-operated channels is enhanced by PKC,[9,10] whereas ATP-sensitive K^+ (K_{ATP}) channels and voltage-dependent K^+ (K_V) channels are inhibited by PKC.[11,12]

Biochemical inhibitors have been widely used to investigate PKC-mediated signal transduction in vivo and in vitro. One method that has been used to study the role of PKC in cellular processes is the inhibition of PKC activity by preincubation with cell-permeable agents that affect PKC activity. However, the usefulness of such PKC inhibitors in intact cells can be limited by nonspecific actions on other proteins besides PKC. For example, calphostin C is a selective inhibitor of PKC but blocks L-type Ca^{2+} channels in frog ventricular cells.[13] Another PKC inhibitor, staurosporine (ST), has been reported to inhibit muscarinic K^+ channels independent of PKC activity[14] and to inhibit $K_V1.3$ channels that were stably expressed in Chinese hamster ovary (CHO) cells.[15] Another potent PKC inhibitor, bisindolylmaleimide [BIM (I)], which is structurally similar to ST, can block $K_V1.5$ channels in CHO cells, acetylcholine-activated K^+ channels in mouse atrial myocytes, and K_V channels in rat mesenteric arterial smooth muscle cells.[16–18] Considering the significance of PKC in vascular function, it is essential to verify the nonspecific actions of PKC inhibitors before experimental data can be interpreted accurately. Therefore, in the present study we investigated the effects of ST on the K_V current in smooth muscle cells freshly isolated from rabbit coronary arteries. We found that ST directly inhibited the K_V current in a voltage-, time-, and use-dependent manner and that the actions of ST were independent of PKC and protein kinase A (PKA) activity. Furthermore, ST shifted the activation curve to more positive potentials, which suggests that ST can interact with K_V channels that are in the closed state as well as inhibit K_V channels that are in open state.

MATERIALS AND METHODS

Cell Isolation

New Zealand White rabbits (1.5−2.0 kg) of either sex were simultaneously anesthetized with pentobarbital sodium

Received for publication November 3, 2004; accepted December 13, 2004.
From the *Department of Physiology and National Research Laboratory for Cellular Signaling, Seoul National University College of Medicine, Seoul, Korea; †Mitochondrial Signaling Laboratory, Department of Physiology and Biophysics, Biohealth Products Research Center, 2020 Cardiovascular Research Institute, College of Medicine, Inje University, Busan, Korea; and ‡Department of Physiology, Konkuk University College of Medicine, Choongju, Korea.

W.S.P. and Y.K.S. contributed equally to this work.
This work was supported by a BK21 Human Life Sciences grant from the Ministry of Education, Korea, and by a National Research Laboratory grant from Ministry of Science and Technology, Korea.
Reprints: Yung E. Earm, MD, PhD, Department of Physiology, College of Medicine, Seoul National University, Seoul 110-799, Korea (e-mail: earmye@snu.ac.kr).

(50 mg/kg) and injected with heparin (100 U/kg) through the ear vein. Arteries were removed and cleaned of connective tissue in the normal Tyrode solution. The arteries were transferred to normal Tyrode solution without $CaCl_2$ (Ca^{2+}-free solution) for 10 minutes and then to 1 mL of Ca^{2+}-free normal Tyrode solution containing papain (1.0 mg/mL), bovine serum albumin (BSA, 1.5 mg/mL), dithioerythritol (DTT, 1.0 mg/mL). After incubation for about 25 minutes, the arteries were transferred to 1 mL of Ca^{2+}-free normal Tyrode solution containing collagenase (2.8 mg/mL), BSA, and DTT for about 20 minutes. After enzyme treatment, the arteries were transferred to Kraft-Brühe (KB) solution. Single smooth muscle cells were obtained by gentle trituration with a fire-polished glass pipette, stored at 4°C, and used on the day of preparation.

Electrophysiology

Currents were recorded from single smooth muscle cells using a whole-cell configuration[19] except for recording of Ca^{2+}-activated K^+ (BK_{Ca}) currents, which were recorded using a cell-attached configuration. An Axopatch-1C amplifier (Axon Instruments) was used for voltage clamping. The patch pipettes were pulled from borosilicate capillaries (Clark Electromedical Instruments, Pangbourne, UK) using a Narishige puller (PP-83, Japan). We used patch pipettes that had a resistance of 2−3 MΩ for the whole-cell configuration and 5 MΩ for cell-attached configuration, respectively, when filled with the pipette solutions described below. Liquid junction potentials between normal Tyrode and pipette solution were offset before the GΩ seal formation was achieved by suction. Seal resistances were in the range of 5 to 10 GΩ. Voltage clamp and data acquisitions were performed using a digital interface (Digidata 1200, Axon Instruments) coupled to an IBM-compatible computer at a sampling rate of 1−2 kHz and filtered at 0.5 kHz for the whole-cell configuration and at a sampling rate of 5 kHz and filtered at 1 kHz for cell-attached configuration. All experiment parameters, such as pulse generation and data acquisition, were controlled using Patchpro software developed by our group.

Solutions and Chemicals

The normal Tyrode solution contained (mM) 143 NaCl, 5.4 KCl, 0.33 NaH_2PO_4, 0.5 $MgCl_2$, 1.8 $CaCl_2$, 5.0 HEPES, and 16.6 glucose, adjusted with NaOH to pH 7.4. The Kraft-Brühe (KB) solution contained (mM) 70 KOH, 50 L-glutamate, 55 KCl, 20 taurine, 20 KH_2PO_4, 3 $MgCl_2$, 0.5 EGTA, 10 HEPES, and 20 glucose, adjusted with KOH to pH 7.3. The pipette solution for recording K_V channels contained (mM) 105 K-aspartate, 25 KCl, 5 NaCl, 1 $MgCl_2$, 4 Mg-ATP, 10 BAPTA, and 10 HEPES, adjusted with KOH to pH 7.25. The pipette solution for the single-channel recording of BK_{Ca} channels contained (mM) 150 KCl, 5 HEPES, 5 EGTA, and 1 $MgCl_2$ adjusted with KOH to pH 7.4. The bath solution for the single-channel recording contained (mM) 150 KCl, 5 HEPES, 5 EGTA, 1 $MgCl_2$, and 3.2 $CaCl_2$ adjusted with KOH to pH 7.4. To block K_{ATP} currents and Ca^{2+}-activated currents, we included 4 mM of Mg-ATP and 10 mM of BAPTA in the pipette solution. For the recording of K_{ATP} currents and inward rectifier K^+ (K_{IR}) currents, the K^+ concentration in the bath solution was increased to 140 mM, replacing Na^+, for amplifying currents. For the recording of K_{ATP} currents, ATP concentration in the pipette solution were decreased to 0.1 mM. In all experiments recording K_V currents, the bath solution contained iberiotoxin (100 nM) to block the BK_{Ca} channel currents. All pharmacological compounds were dissolved in distilled water or in dimethyl sulfoxide (DMSO) to make stock solutions, which were diluted in the normal Tyrode solution to the concentration used. The concentration of DMSO in the final dilution was less than 0.1%, a level at which DMSO had no effect on the current recording. PKA inhibitor peptide (PKA-IP) was purchased from Tocris Company. ST, chelerythrine, and iberiotoxin were purchased from Sigma Chemical Co.

Data Analysis

Origin 6.0 software (Microcal Software, Inc, Northampton, MA) was used for data analysis. Interaction kinetics between drugs and channels was described on the basis of a first-order blocking scheme, as described previously.[20] The apparent affinity constant (K_d) and Hill coefficient (n) were obtained by fitting concentration-dependence data to the following Hill equation:

$$f = 1/\{1 + (K_d/[\mathrm{D}])^n\} \quad (1)$$

in which f is the fractional inhibition ($f = 1 - I_{drug}/I_{control}$) at the test potential, and [D] represents different drug concentrations.

The activation kinetics were calculated by fitting the data to a single exponential, which was considered to be the dominant time constant of activation.[21] The time courses of the current during inactivation were fitted to a single exponential function for the control condition or to a double-exponential function with the fast component regarded as the effect of the drug. The apparent rate constants of association (k_{+1}) and dissociation (k_{-1}) were obtained from the following equation:

$$1/\tau_D = k_{+1}[\mathrm{D}] + k_{-1} \quad (2a)$$

$$K_d = k_{-1}/k_{+1} \quad (2b)$$

where τ_D is the drug-induced time constant.

The experimental points were calculated as:

$$\text{Normalized } I = (I - I_c)/(I_{max} - I_c) \quad (3)$$

where I_{max} represents the maximal current measured, and I_c represents a nonzero current that was not inactivated. We eliminated this nonzero residual current by subtracting it from the actual values.

Activation curves were fitted with the following Boltzmann equation:

$$y = 1/\{1 + \exp\,(-(V - V_{1/2})/k)\} \quad (4)$$

where k represents the slope factor, V represents the test potential, and $V_{½}$ is the voltage at which the conductance was half-maximal. The steady-state voltage dependence of inactivation was investigated using a 2-pulse voltage protocol; currents were measured with a 600-millisecond test potential to +40 mV, and 7-second preconditioning pulses were varied

from −60 to +50 mV (in 10-mV steps) in the absence and presence of drugs. The resulting steady-state inactivation data were fitted with Boltzmann equation:

$$y = 1/\{1 + \exp((V - V_{1/2})/k)\} \quad (5)$$

where V is the preconditioning potential, $V_{½}$ represents the potential corresponding to the half-inactivation point, and k represents the slope value.

To investigate the voltage dependence of the fractional inhibition by a drug, we calculated the fractional inhibition at each test potential above the initial potential (−40 mV) of activation. Using the resulting data, the voltage dependence of the fractional inhibition was fitted with a Woodhull equation[22]:

$$f = [D]/\{[D] + K_d(0) \times \exp(-z\delta FV/RT)\} \quad (6)$$

where $K_d(0)$ is the apparent affinity at 0 mV (the reference voltage), z is the charge valence of the drug, δ is the fractional electrical distance (ie, the fraction of the transmembrane electric field sensed by a single charge at the receptor site), F is the Faraday constant, R is the gas constant, and T is the absolute temperature. In this study, we used 25.4 mV as the value of RT/F at 22°C.

Single-channel activities were presented as NP_O, where N is the number of channels and P_O is the open probability.

Data are presented as the mean ± SE of the mean. Student t test was used for the test of significance ($P < 0.05$).

RESULTS

Inhibition of K_V Current by Staurosporine

Figure 1 illustrates the effects of ST on K_V currents in rabbit coronary arterial smooth muscle cells. Under the control conditions (Fig. 1A), the K_V current rose rapidly to a peak and then displayed slow inactivation during a 600-millisecond depolarizing pulse, as reported previously.[23] The K_V current was diminished in the presence of 1 μM ST (Fig. 1B). The steady state was reached within 1 minute of switching to a solution containing 1 μM ST. Panels C and D in Figure 1 show the peak and steady state of the current–voltage (I-V) relationship of K_V currents in the absence and presence of ST, respectively. The I-V relationship indicates that the magnitudes of both the peak and the steady-state K_V currents were decreased to a similar extent by ST. The washout of ST by perfusion of drug-free solution occurred within 5 minutes, after which the K_V current recovered to 87.1 ± 0.3% (n = 5) of that under control conditions.

Differential Dose-Dependent Inhibition of K_V Current by Staurosporine

Figure 2 illustrates the concentration dependence of the effects of ST on the K_V current. Examples of inhibition of the K_V current by 0.3, 1.0, and 3.0 μM ST are presented in Figure 2A. As was illustrated in Figure 1, the inhibition of K_V current by ST was similar for both the peak and the steady-state K_V

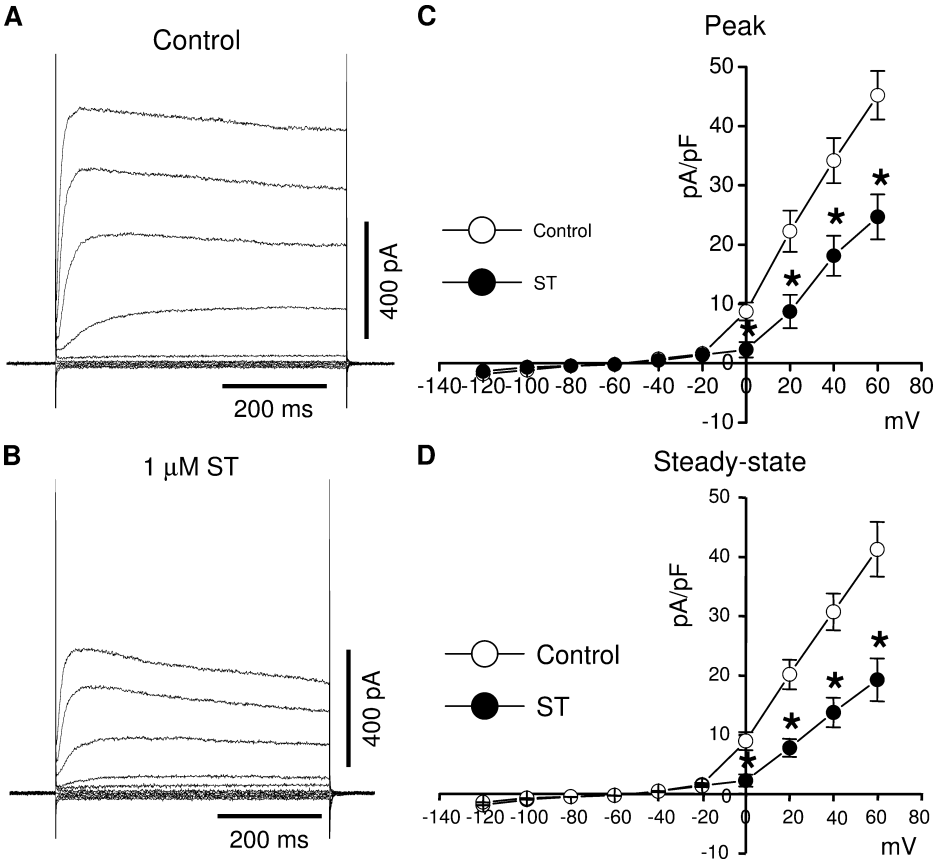

FIGURE 1. Inhibitory effects of ST on the voltage-dependent K^+ (K_V) currents in rabbit coronary arterial smooth muscle cells. A and B, Superimposed current traces were elicited by 600-millisecond pulses between −120 mV and +60 mV from a holding potential of −60 mV in steps of 20 mV under control conditions (A) and in the presence of 1 μM ST (B). C, Current–voltage (I-V) relationships of the peak K_V currents in the absence (○) and presence (●) of 1 μM ST (n = 5). D, I-V relationships of the steady-state K_V currents in the absence (○) and presence (●) of 1 μM ST (n = 5). Peak K_V currents were measured within 70 milliseconds after the pulses were applied, and steady-state K_V currents were measured at the end of 600-millisecond pulses. *$P < 0.05$.

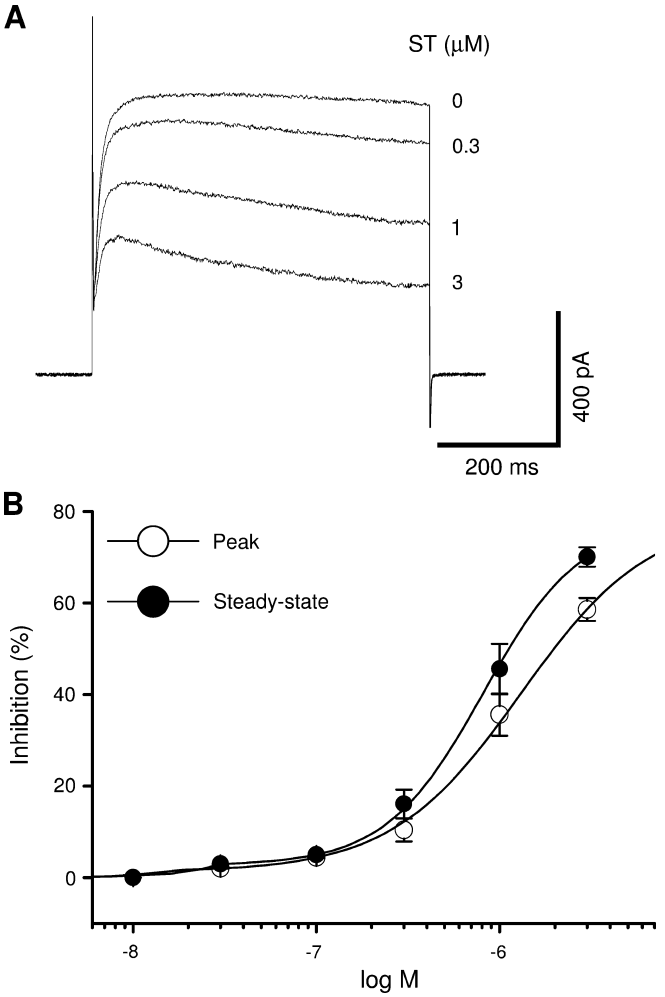

FIGURE 2. Concentration dependence of the inhibition of K_V currents by ST. A, Superimposed currents were elicited by applying 600-millisecond depolarizing pulses from a holding potential of −60 mV to +40 mV. The traces of the currents obtained in the absence and presence of 0.3, 1, and 3 μM ST. The average concentration dependences of K_V current inhibition by ST are shown in B. The drug-induced inhibition was measured at peak (○) and at steady state (●) and normalized to the current in the absence of each drug. The normalized currents were fitted with the Hill equation, which yielded a K_d value of 1.35 ± 0.42 μM and a Hill coefficient of 1.21 ± 0.09 (n = 4).

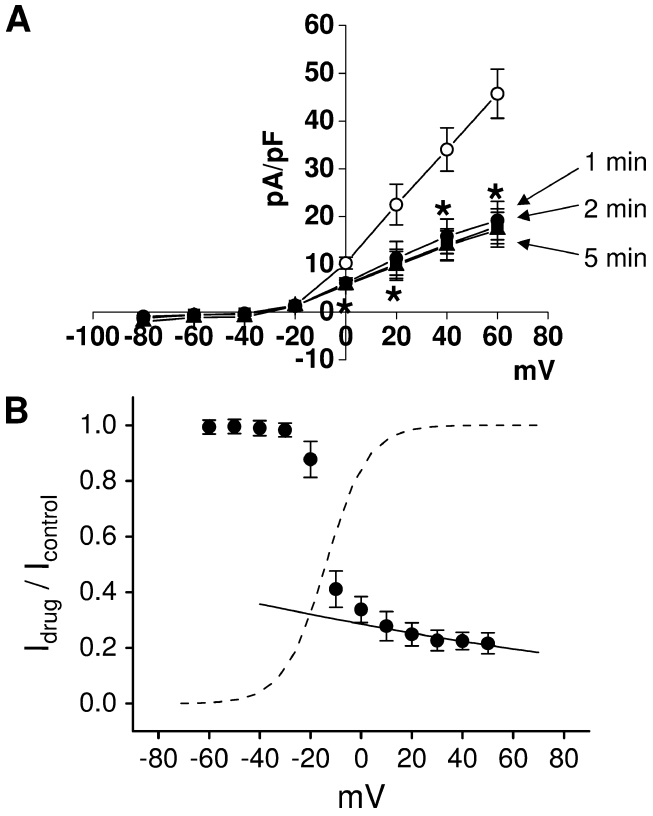

FIGURE 3. Voltage dependence of the K_V current inhibition induced by ST. A, I-V relationships (all n = 4) were obtained by the following protocol: from a holding potential of −60 mV, a first control step (400 milliseconds) followed by application of staurosporine (at holding potential of −60 mV) over 1 minute without application of step voltage, followed by a series of steps (to the same voltage as the control one) with an interval between steps of 6 seconds. *$P < 0.05$. B, Normalized inhibition shown as relative current expressed as $I_{drug}/I_{control}$ from the data shown in Figure 1D, at each potential (n = 5). The dotted line represents the activation curve of the K_V currents examined in this experiment under control conditions (see Fig. 5) and shows the voltage dependence of ST. For potentials positive to +10 mV, the voltage dependence was fitted (solid line) with a Woodhull equation, which yielded δ = 0.21 ± 0.04 (n = 5).

current. For the steady-state inhibition, a nonlinear least-squares fit of the Hill equation to the concentration–response data at +40 mV yielded a K_d value of 1.35 ± 0.42 μM and a Hill coefficient of 1.21 ± 0.09.

Voltage Dependence of Drug-Channel Interactions

The I-V relationships for the inhibition of steady-state K_V current according to time indicated that ST reduces the K_V current over the entire range of voltages at which K_V channels are open (Fig. 3A). To quantify the effects of voltage on the interaction between the ST and K_V channels, the relative current ($I_{drug}/I_{control}$) was plotted as a function of the membrane potential (Fig. 3B). The dotted line in Figure 3B represents the activation curve of K_V channels under control conditions. The K_V current was activated at about −40 mV, and the channel conductance was fully saturated above +10 mV. In the presence of 1 μM ST, the degree of inhibition of K_V current increased steeply between −20 and +10 mV (Fig. 3B), which corresponds to the range of voltages in which K_V channels are open.

An additional small degree of inhibition with a shallow (but meaningful) voltage dependence was detected at the voltages greater than +10 mV, despite the fact that K_V channels are fully activated at such voltages. Under the assumption that ST interacts intracellularly with K_V channels, we investigated these effects by using a simple Woodhull equation (see Equation 6 in the Methods section) to fit the data at potentials

more positive than +10 mV. The solid line in Figure 3B represents the fitted curve, for which the value of δ was 0.21 ± 0.04 in the presence of ST.

Concentration Dependence of the Time Course of K_V Channel Inhibition

We investigated the kinetics of the inhibition of K_V current by ST. The activation process was fitted with a single exponential function. Under control conditions, the dominant time constant for activation of the K_V current was 13.08 ± 0.13 milliseconds (n = 6) elicited by 600 milliseconds of depolarizing pulses from a holding potential of −60 mV to +40 mV. In the presence of 1 μM ST, the time constant was 13.17 ± 0.21 milliseconds (n = 5), which suggests that ST did not significantly modify the activation kinetics of K_V channels.

However, as shown in Figure 2A, in the presence of ST, the decay in the K_V current was accelerated in a concentration-dependent manner. The control K_V current decayed slowly and partially, with a time constant of 1036 ± 36 milliseconds at +40 mV (calculated by fitting a single exponential function), which was attributed to intrinsic inactivation.[23,24] Therefore, we used a double-exponential function to fit the data at voltages positive to +40 mV in the presence of ST, thereby obtaining 2 time constants. The time constant for the fast falling phase was considered to represent the time constant of the development of a drug-induced blockade of K_V current (τ_D), whereas the time constant for the slow phase reflected partial inactivation. In Figure 4, the reciprocal of the time constant for the inhibition of K_V current at +40 mV was plotted against the concentration of ST. The straight lines represent the least-squares fit of Equation 2a. Using this approach, we calculated the association constant k_{+1} as 0.63 ± 0.05 μM^{-1} s^{-1}, and the dissociation constant k_{-1} as 0.91 ± 0.07 s^{-1}. Under the previous assumption of a first-order reaction between drug and receptor, we calculated the apparent K_d from Equation 2b: the derived K_d value for ST was 1.45 ± 0.02 μM. These results correspond closely with the K_d value that was calculated by fitting the concentration–response curves (Fig. 2).

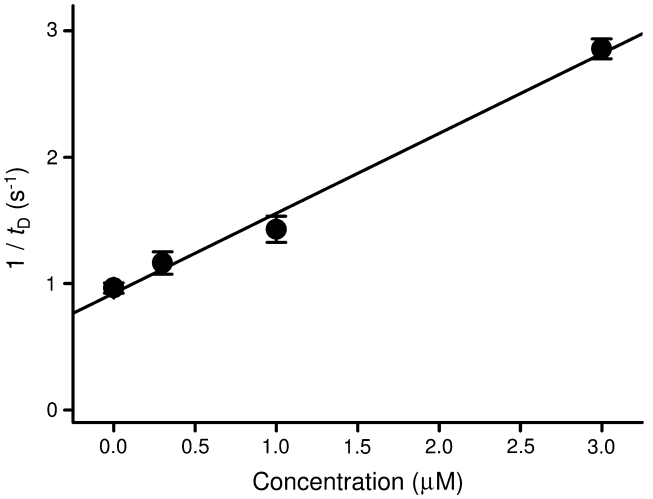

FIGURE 4. Time constant of inhibition as a function of the drug concentration. The drug-induced time constants (τ_D) of apparent current decay were obtained by single- (control) or double (in the presence of different concentrations of ST)-exponential fitting. The reciprocals of τ_D obtained were plotted against the drug concentration at +40 mV. The solid line represents the least-squares fit to the first-order clocking scheme: $1/\tau_D = k_{+1}[D] + k_{-1}$. An apparent association rate constant (k_{+1}) of 0.63 ± 0.05 $\mu M^{-1}s^{-1}$ and dissociation rate constant (k_{-1}) of 0.91 ± 0.07 s^{-1} for ST (n = 4) were obtained from the slope and intercept value of the fitted line.

Effects of Staurosporine on the Activation and Steady-State Inactivation of K_V Channels

The voltage dependence of activation and steady-state inactivation was evaluated to determine whether the inhibition of K_V current by ST was caused by a shift in the activation and/or inactivation curves. Activation curves were constructed using the tail current in a typical 2-pulse protocol, and the data were fitted with a Boltzmann function (Equation 4 in the Methods section). Figure 5A shows the voltage dependence of activation under control conditions and in the presence of 1 μM ST. The application of 1 μM ST caused a significant positive shift in the activation curve. Half-maximal activation was shifted by +14 mV in the presence of 1 μM ST, but the slope of the activation curve was not altered (Fig. 5A). The potential of the half-maximal activation ($V_{½}$) and slope value (k) were −14.89 ± 0.79 mV and 9.51 ± 0.69, respectively, under control conditions; −0.42 ± 0.78 mV and 10.07 ± 0.69, respectively, in the presence of 1 μM ST.

ST did not shift the voltage dependence of inactivation (Fig. 5B). After fitting to a Boltzmann equation, (Equation 5 in the Methods section), the potential of the half-inactivation ($V_{½}$) and slope value (k) were −34.59 ± 0.41 mV and 9.79 ± 0.30, respectively, under control conditions; −35.15 ± 0.28 mV and 10.84 ± 0.25, respectively, in the presence of 1 μM ST.

Effects of Staurosporine on Recovery Kinetics of K_V Channels

We investigated recovery kinetics using a double-pulse protocol in which the interpulse interval was varied from 20 milliseconds to 7 seconds. Figure 6 shows the peak current amplitudes normalized to the maximal peak current. The data were fitted with a single exponential function with recovery time constants of 856.95 ± 282.61 milliseconds under control conditions and 1315.54 ± 100.02 milliseconds in the presence of 1 μM ST.

The significant increase in the recovery times in the presence of ST suggests that the dissociation rate of ST was lower than the transition rate between the open and the closed (or resting) state of the K_V channels under control conditions, which may suggest that the blockade of the K_V current by ST was use-dependent.

Effects of Other Protein Kinase Inhibitors on the Inhibition of K_V Channels by Staurosporine

To investigate whether the inhibition of the K_V current by ST resulted from an inhibition of PKC and/or PKA, we tested the effects of other PKC and PKA inhibitors on the K_V current. Chelerythrine (3 μM), a general PKC blocker, did not

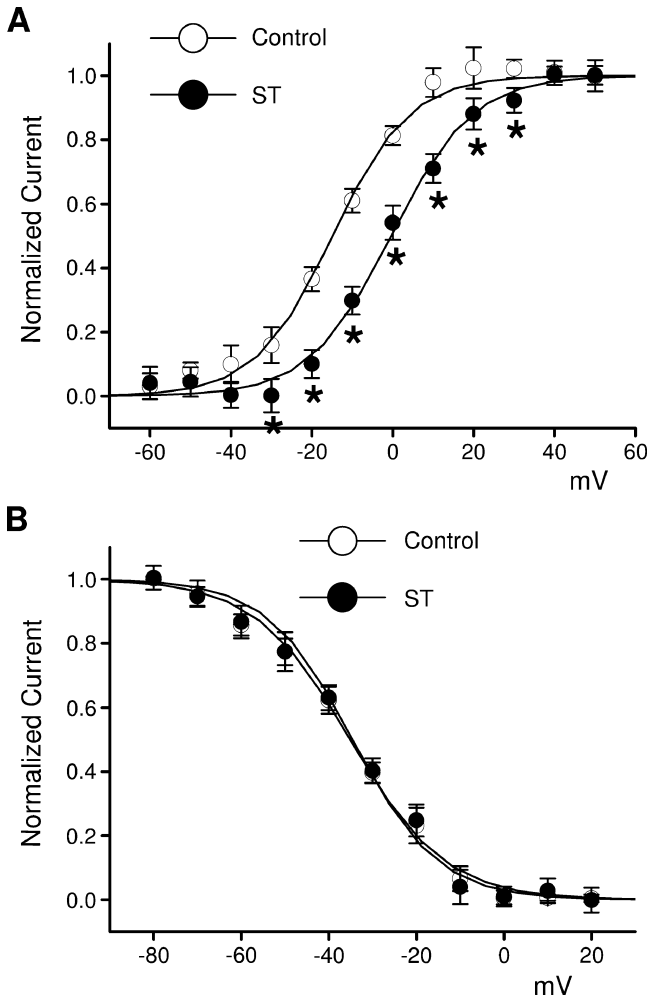

FIGURE 5. Effects of ST on the activation and the steady-state inactivation of K_V currents. A, Activation curves under control conditions (○) and in the presence of 1 μM ST (●, n = 5); the lines are the best fit of a Boltzmann function. The activation curves were obtained from a double-pulse protocol from a holding potential of −60 mV. The channels were activated by the application of a short depolarizing pulse to values between −60 and +50 mV in steps of 10 mV. The activating pulse in the first double-pulse step of this protocol was 30–100 milliseconds, according to the activation time course of Figure 1. The second pulses stepped the membrane potential to −40 mV, and the peak value of the tail current was measured. The normalized current amplitude was considered to be an estimate for channel activation. $*P < 0.05$. B, Steady-state inactivation curves under control conditions (○) and in the presence of 1 μM ST (●, n = 4). The currents were activated by a test step to +40 mV after a 7-second conditioning prepulse at different voltages. The steady-state current amplitude in the test pulse was normalized to the peak amplitude after a prepulse potential. Data were fit to the Boltzmann equation, represented as smooth lines.

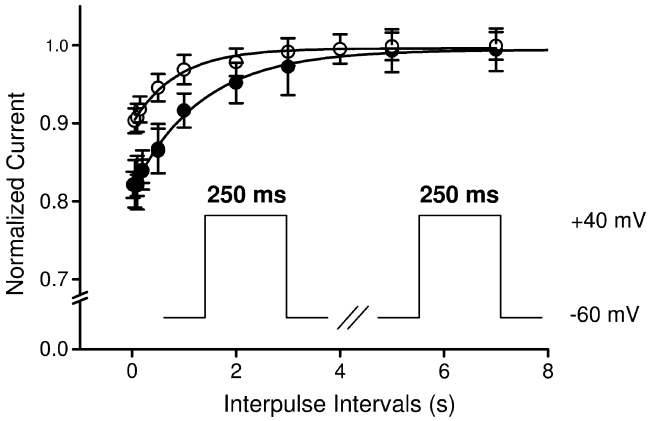

FIGURE 6. Analysis of the recovery of K_V currents from ST block. To measure the degree of recovery, a double-pulse protocol was applied, as shown in the inset. The first prepulse of a 250-millisecond depolarizing potential of +40 mV from a holding potential of −60 mV was followed by the second identical pulse after an increase in the time interval (from 20 milliseconds to 7 seconds). The peak amplitude of the current elicited by the second test pulses were plotted as a function of the pulse interval after being normalized to the peak amplitude of the current elicited by the first prepulses. The solid line represents a typical example of the recovery kinetics of K_V current obtained under control condition (○, n = 4) and in the presence of 1 μM ST (●, n = 4). The curves were obtained by fitting the plotted data to a single exponential function, yielding recovery time constants of 856.95 ± 282.61 milliseconds under control condition, 1315.54 ± 100.02 milliseconds in the presence of 1 μM ST.

significantly alter the effects of 1 μM ST on the K_V current (Fig. 7A). Similarly, the general PKA inhibitor, PKA inhibitor peptide (PKA-IP, 5 μM in the pipette solution), did not significantly alter the effects of 1 μM ST on the K_V current (Fig. 7B). The application of chelerythrine or PKA-IP alone had little effect on the K_V current, whereas the application of 1 μM ST together with chelerythrine or PKA-IP reduced the K_V current by 41.12 ± 2.11% and 40.68 ± 2.43%, respectively. This reduction in the magnitude of the K_V current by ST in the presence of chelerythrine or PKA-IP was not different from the magnitude of inhibition of the K_V current by ST alone (45.6 ± 2.5%; Figs. 2 and 7C). These results suggest that ST did not inhibit K_V current via an action on PKC or PKA but that this drug acted directly on K_V channels. We also tested the effect of ST on K_V currents in the absence of pipette ATP. However, as shown in Figure 7D, the presence or absence of ATP inside the pipette did not influence the blocking effect of ST on K_V channels. These results suggest that the effect of ST occurs in a phosphorylation-independent manner.

Effects of Staurosporine on Other K^+ Channels

Coronary arterial smooth muscle cells have several other types of K^+ channels, including K_{ATP}, BK_{Ca}, and K_{IR} channels.[25–27] We tested the effects of 1 μM ST on each of the aforementioned types of K^+ channels. To address the K_{ATP} channels, whole-cell currents were recorded at a holding potential of −60 mV to minimize the activity of K_V and BK_{Ca} channels (cell was dialyzed with BAPTA) and the concentration of intracellular ATP was lowered to 0.1 mM. To amplify the magnitude of the K_{ATP} current, we increased the concentration of extracellular K^+ to 140 mM and applied the K_{ATP}

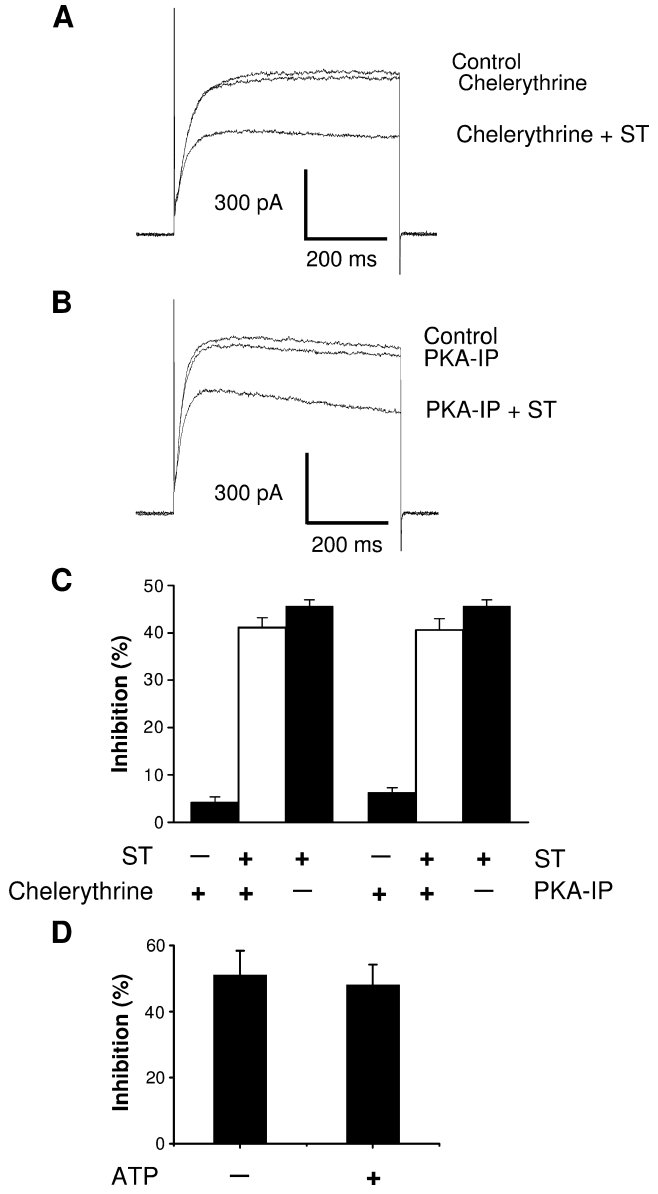

FIGURE 7. Effects of PKC and PKA inhibitors on the ST-induced inhibition of K_V currents. A, Current traces under control conditions, and in the presence of 3 μM chelerythrine, and with the additional application of 1 μM ST (n = 3), with a depolarization pulse to +40 mV from a holding potential of −60 mV. B, Similar current traces under control conditions, and with 5 μM PKA-IP, and with the additional application of 1 μM ST (n = 4). These results were summarized in C. D, Effects of pipette ATP on the ST-induced inhibition of K_V currents. Current traces in the presence (n = 4) and absence (n = 3) of pipette ATP are obtained by depolarization pulse to +40 mV from a holding potential of −60 mV.

channel opener pinacidil (10 μM). The effect of pinacidil on K_{ATP} channels is illustrated in Figure 8A. To confirm that the pinacidil-induced current was the K_{ATP} current, we demonstrated that inward current could be reversed rapidly back to control levels by the application of the sulfonylurea glibenclamide (10 μM). ST had no effect on the K_{ATP} current, which was 10.73 ± 1.25 pA/pF and 9.99 ± 1.00 pA/pF under control conditions and in the presence of 1 μM ST, respectively (Fig. 8A, right panel; n = 4).

To record the K_{IR} current, we used an approach similar to that used to record the K_{ATP} current, except that we included intracellular ATP (4 mM) to minimize the K_{ATP} current. As illustrated in Figure 8B, ST had no effect on the K_{IR} current, which was 8.98 ± 1.03 pA/pF and 8.78 ± 0.92 pA/pF under control conditions and in the presence of 1 μM ST, respectively (Fig. 8B, right panel; n = 4).

The effects of ST on BK_{Ca} channels were studied in the cell-attached configuration. BK_{Ca} channel activity was not affected by ST: thus NP_O at +60 mV was 0.02296 ± 0.0018 and 0.02301 ± 0.0021 under control conditions and in the presence of 1 μM ST, respectively (Fig. 8C; n = 3).

DISCUSSION

In the present study, we investigated the effects of ST on K_V channels in rabbit coronary arterial smooth muscle cells and found that ST inhibited K_V channels in a voltage-, time-, and use-dependent manner. In addition, the voltage-dependent inactivation curves of the K_V channels were not significantly altered by ST, whereas the activation curve was shifted toward more positive potentials.

In the present study, ST appeared to inhibit the K_V current directly rather than acting via PKC or PKA. The K_d value of ST (1.35 μM) was much greater than the half-inhibition value for PKC inhibition (0.7 nM for ST[28]). Moreover, the blockade of the K_V current in vascular smooth muscle cells requires PKC activation[12] rather than inhibition. In addition, the selective PKC inhibitor chelerythrine (used at 3 μM in the present study; half-inhibition value of 0.66 μM[29]), affected neither the K_V current under control conditions nor the inhibitory effects of ST on the K_V current (see Fig. 7A).

The half-inhibition concentration of ST for PKA is 7 nM. In our experiments, the half-inhibition concentration of ST for the K_V current was 1.3 μM, which reflects a much greater degree of inhibition than that of ST on PKA activity. Therefore, we tested the effect of PKA on the K_V current by applying a specific PKA inhibitor peptide (5 μM PKA-IP) but found that inhibition of PKA affected neither the K_V current nor the inhibitory effects of ST (see Fig. 7B). These results strongly suggest that ST acted directly on the K_V channels in coronary smooth muscle cells to inhibit K_V current independently of PKC or PKA.

In the present study, ST did not significantly alter the activation time constant of K_V channels in coronary arterial smooth muscle cells; this suggests that ST does not block K_V channels in the closed or resting state in native cells from coronary arteries. This concurs with previous reports on the effect of ST on heterologously expressed $K_V1.3$ channels[15] and also with the results of studies of the effects of BIM (I) on K_V channels from mesenteric arteries[18] and heterologously expressed $K_V1.5$ channels.[16] However, we found in the present study that ST accelerated the rate of K_V current decay. The time constant of the fast component of inactivation in the presence of 1 μM ST was 1.5-fold greater than that under control

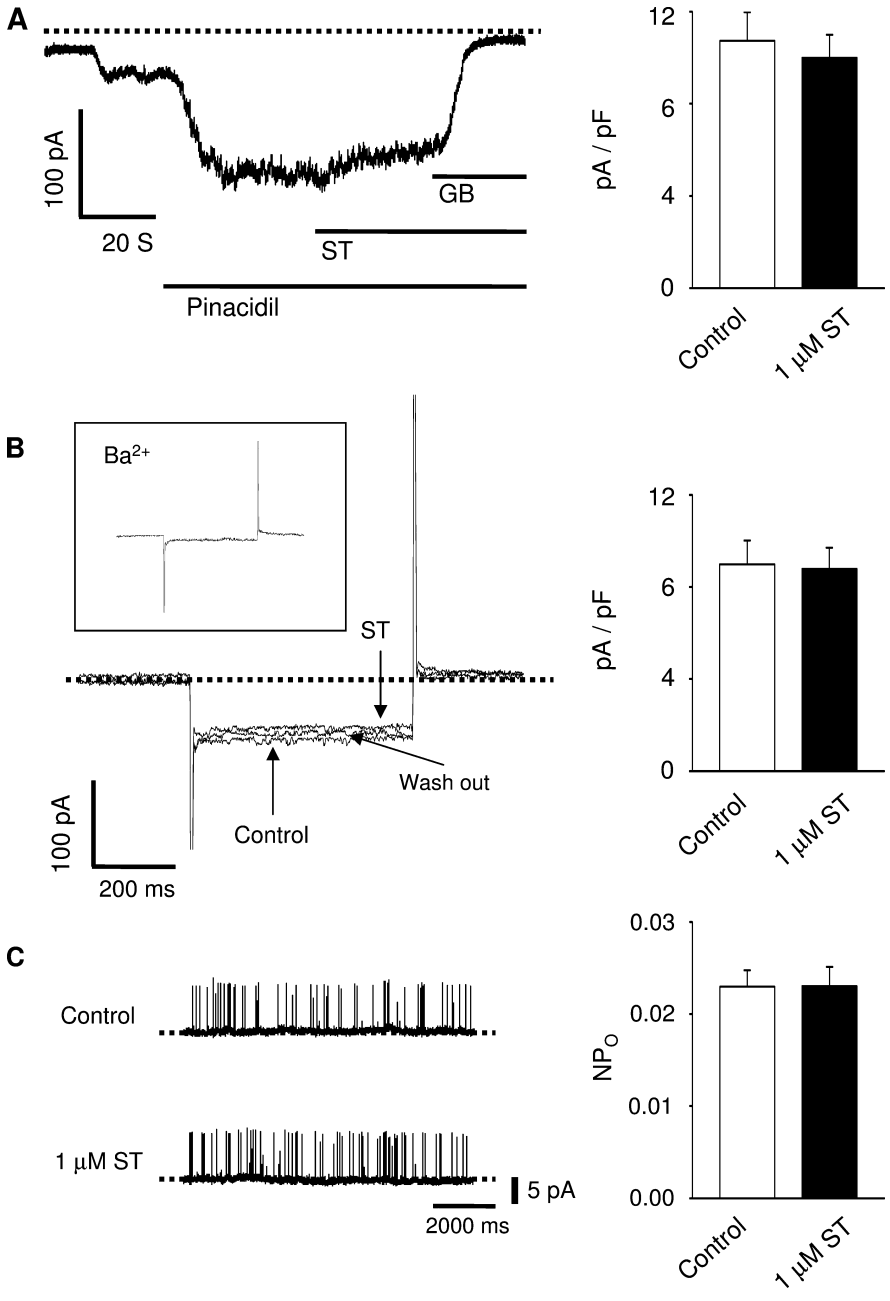

FIGURE 8. Effects of ST on other K^+ currents. A, Left panel shows K_{ATP} currents with ST application after amplification by 140 mM K^+ in the bath solution and the application of 10 μM pinacidil. Right panel shows the current density of K_{ATP} channels in the absence and presence of ST. B, Left panel shows superimposed inward rectifier K^+ currents under the control conditions and during the application of ST, which is summarized as current density in the right panel. Currents were elicited by applying 400-millisecond hyperpolarizing pulses from a holding potential of −60 mV to −120 mV. Inward rectifier K^+ currents were confirmed later with inhibition by 40 μM Ba^{2+} (in box). C, Left panel shows Ca^{2+}-activated K^+ (BK_{Ca}) currents recorded in cell-attached configuration. Current traces recorded with 150 mM KCl in the bath and pipette solutions at +60 mV. The bath solution contained 3.2 mM $CaCl_2$ (pCa = 6.5 according to the Fabiato and Fabiato formula). NP_O was calculated and summarized in the right panel.

conditions; in the presence of 3 μM ST, the time constant was 3-fold greater than the control value. These results suggest that ST may have blocked the pore of K_V channels that were in the open state.

Choi et al[15] found that ST acted on $K_V1.3$ channels in CHO cells independent of PKC and PKA. In that study, ST did not affect the peak amplitude of the $K_V1.3$ current but enhanced the rate of current decay in a concentration-dependent manner. However, our data showed that ST inhibited both the peak amplitude of K_V currents and the steady-state current in freshly isolated coronary arterial smooth muscle cells. This difference between the results obtained in the present study and those of Choi et al[15] might be caused by the use of different model systems (CHO cells versus freshly isolated coronary arterial smooth muscle cells).

The inhibitory effects of ST on the K_V current were clearly voltage dependent. Within the voltage range of K_V channel activation, the inhibition of K_V current by ST increased greatly, thus providing strong evidence that a K_V channel must be open for it to be inhibited by ST. Moreover, there was a shallow voltage dependence for inhibition by ST in the voltage range at which K_V channels are activated fully. Woodhull[22] explained this phenomenon by means of a simple model. According to the Woodhull model, if a positively charged drug moves into the transmembrane electric field from the inside, then inhibition should increase on depolarization

because of the electrostatic repulsion between the positively charged drug and the membrane depolarizing potential. This would occur in the voltage range at which channels are in the open state and may also occur in the voltage range at which channels are activated fully. The pK_a of ST is ~10, which means that in physiological solutions (pH ~7.4) ST exists mainly in a positively charged form. Therefore, the value of $\delta = 0.21$ for the voltage dependence of the apparent K_d of ST can be interpreted to indicate that the positively charged amine senses about 20% of the electrical field. This interpretation has been proposed in previous studies with antiarrhythmic agents[30,31] or with TEA,[32] which reported δ values.

ST includes 5-aromatic-ring motifs and protonated ammonium ions, which may constitute the key features of ST that allow this drug to block K_V channels. Previous reports have suggested that protonated ammonium ions inhibit K_V channels only after the channel activation gates have opened and that hydrophobic interactions between the drugs and channels determine the stability and affinity of binding.[20,33–36] At a physiological pH, ST has protonated tertiary ammonium ions, which would facilitate an association with a K^+ coordinating site within the channel cavity.[37,38]

Although ST did not affect the voltage dependence of K_V channel inactivation, effects of ST on the voltage dependence of activation were noticeable: ST shifted activation to more positive potentials, which is different from other reports on the effects of ST. These results suggest that ST changed the voltage sensitivity of K_V channels, which implies ST can interact with the K_V channel while it is in the closed state (which resembles the effect of 4-AP on K_V channels[39]) as well as blocking the cavity of K_V channels that are in the open state.

In conclusion, in the present study we found that ST directly inhibited the K_V current in rabbit coronary arterial smooth muscle cells. Therefore, caution is required when using ST (which inhibits PKC) in functional studies of modulation of ion channels by protein phosphorylation.

REFERENCES

1. Hug H, Sarre TF. Protein kinase C isoenzymes: divergence in signal transduction? *Biochem J.* 1993;291:329–343.
2. Nishizuka Y. Studies and prospectives of the protein kinase C family for cellular regulation. *Cancer.* 1989;63:1892–1903.
3. Nishizuka Y. Protein kinase C and lipid signaling for sustained cellular responses. *FASEB J.* 1995;9:484–496.
4. Steinberg SF, Goldberg M, Rybin VO. Protein kinase C isoform diversity in the heart. *J Mol Cell Cardiol*. 1995;27:141–153.
5. Sugden PH, Bogoyevitch MA. Intracellular signalling through protein kinases in the heart. *Cardiovasc Res*. 1995;30:478–492.
6. Eto M, Kitazawa T, Yazawa M, et al. Histamine-induced vasoconstriction involves phosphorylation of a specific inhibitor protein for myosin phosphatase by protein kinase C α and δ isoforms. *J Biol Chem*. 2001;276: 29072–29078.
7. Li PF, Maasch C, Haller H, et al. Requirement for protein kinase C in reactive oxygen species-induced apoptosis of vascular smooth muscle cells. *Circulation*. 1999;100:967–973.
8. Watanabe T, Pakala R, Katagiri T, et al. Synergistic effect of urotensin II with serotonin on vascular smooth muscle cell proliferation. *J Hypertens*. 2001;19:2191–2196.
9. Albert AP, Large WA. Activation of store-operated channels by noradrenaline via protein kinase C in rabbit portal vein myocytes. *J Physiol*. 2002;544:113–125.
10. Keef KD, Hume JR, Zhong J. Regulation of cardiac and smooth muscle Ca^{2+} channels (Ca_V1.2a,b) by protein kinases. *Am J Physiol Cell Physiol*. 2001;281:C1743–C1756.
11. Kubo M, Quayle JM, Standen NB. Angiotensin II inhibition of ATP-sensitive K^+ currents in rat arterial smooth muscle cells through protein kinase C. *J Physiol*. 1997;503:489–496.
12. Shimoda LA, Sylvester JT, Sham JS. Inhibition of voltage-gated K^+ current in rat intrapulmonary arterial myocytes by endothelin-1. *Am J Physiol*. 1998;274:L842–L853.
13. Hartzell HC, Rinderknecht A. Calphostin C, a widely used protein kinase C inhibitor, directly and potently blocks L-type Ca channels. *Am J Physiol*. 1996;270:C1293–C1299.
14. Lo CF, Breitwieser GE. Protein kinase-independent inhibition of muscarinic K^+ channels by staurosporine. *Am J Physiol.* 1994;266:C1128–C1132.
15. Choi JS, Hahn SJ, Rhie DJ, et al. Staurosporine directly blocks K_V1.3 channels expressed in Chinese hamster ovary cells. *Naunyn Schmiedebergs Arch Pharmacol*. 1999;359:256–261.
16. Choi BH, Choi JS, Jeong SW, et al. Direct block by bisindolylmaleimide of rat K_V1.5 expressed in Chinese hamster ovary cells. *J Pharmacol Exp Ther.* 2000;293:634–640.
17. Cho H, Youm JB, Earm YE, et al. Inhibition of acetylcholine-activated K^+ current by chelerythrine and bisindolylmaleimide I in atrial myocytes from mice. *Eur J Pharmacol*. 2001;424:173–178.
18. Kim A, Bae YM, Kim J, et al. Direct block by bisindolylmaleimide of the voltage-dependent K^+ currents of rat mesenteric arterial smooth muscle. *Eur J Pharmacol*. 2004;483:117–126.
19. Hamill OP, Marty A, Neher E, et al. Improved patch-clamp techniques for high-resolution current recording from cells and cell-free membrane patches. *Pflugers Arch*. 1981;391:85–100.
20. Snyders DJ, Yeola SW. Determinants of antiarrhythmic drug action. Electrostatic and hydrophobic components of block of the human cardiac hK_V1.5 channel. *Circ Res*. 1995;77:575–583.
21. Snyders DJ, Tamkun MM, Bennett PB. A rapidly activating and slowly inactivating potassium channel cloned from human heart. *J Gen Physiol*. 1993;101:513–543.
22. Woodhull AM. Ionic blockage of sodium channels in nerve. *J Gen Physiol*. 1973;61:687–708.
23. Roberds SL, Knoth KM, Po S, et al. Molecular biology of the voltage-gated potassium channels of the cardiovascular system. *J Cardiovasc Electrophysiol*. 1993;4:68–80.
24. Nelson MT, Quayle JM. Physiological roles and properties of potassium channels in arterial smooth muscle. *Am J Physiol*. 1995;268:C799–C822.
25. Dart C, Standen NB. Adenosine-activated potassium current in smooth muscle cells isolated from the pig coronary artery. *J Physiol.* 1993;471: 767–786.
26. Quayle JM, Dart C, Standen NB. The properties and distribution of inward rectifier potassium currents in pig coronary arterial smooth muscle. *J Physiol*. 1996;494:715–726.
27. Toro L, Vaca L, Stefani E. Calcium-activated potassium channels from coronary smooth muscle reconstituted in lipid bilayers. *Am J Physiol*. 1991;260:H1779–H1789.
28. Toullec D, Pianetti P, Coste H, et al. The bisindolylmaleimide GF 109203X is a potent and selective inhibitor of protein kinase C. *J Biol Chem*. 1991;266:15771–15781.
29. Herbert JM, Augereau JM, Gleye J, et al. Chelerythrine is a potent and specific inhibitor of protein kinase C. *Biochem Biophys Res Commun*. 1990;172:993–999.
30. Snyders DJ, Knoth KM, Roberds SL, et al. Time-, voltage-, and state-dependent block by quinidine of a cloned human cardiac potassium channel. *Mol Pharmacol*. 1992;41:322–330.
31. Valenzuela C, Delpon E, Franqueza L, et al. Class III antiarrhythmic effects of zatebradine: Time-, state-, use-, and voltage-dependent block of hK_V1.5 channels. *Circulation*. 1996;94:562–570.
32. Yellen G, Jurman ME, Abramson T, et al. Mutations affecting internal TEA blockade identify the probable pore-forming region of a K^+ channel. *Science*. 1991;251:939–942.
33. del Camino D, Holmgren M, Liu Y, et al. Blocker protection in the pore of a voltage-gated K^+ channel and its structural implications. *Nature*. 2000;403:321–325.

34. French RJ, Shoukimas JJ. Blockage of squid axon potassium conductance by internal *tetra-N*-alkylammonium ions of various sizes. *Biophys J*. 1981;34:271–291.
35. Heginbotham L, MacKinnon R. The aromatic binding site for tetraethylammonium ion on potassium channels. *Neuron*. 1992;8: 483–491.
36. Hoshi T, Zagotta WN, Aldrich RW. Biophysical and molecular mechanisms of *Shaker* potassium channel inactivation. *Science*. 1990;250: 533–538.
37. Doyle DA, Morais Cabral J, Pfuetzner RA, et al. The structure of the potassium channel: molecular basis of K^+ conduction and selectivity. *Science*. 1998;280:69–77.
38. Roux B, MacKinnon R. The cavity and pore helices in the KcsA K^+ channel: electrostatic stabilization of monovalent cations. *Science*. 1999; 285:100–102.
39. Remillard CV, Leblanc N. Mechanism of inhibition of delayed rectifier K^+ current by 4-aminopyridine in rabbit coronary myocytes. *J Physiol*. 1996; 491:383–400.

